Rotational Resonance NMR Study of the Active Site Structure in Bacteriorhodopsin: Conformation of the Schiff Base Linkage†

Lynmarie K. Thompson,‡,§ Ann E. McDermott,‡,∥ Jan Raap,⊥ C. M. van der Wielen,⊥ Johan Lugtenburg,⊥ Judith Herzfeld,+ and Robert G. Griffin*,‡

Department of Chemistry and Francis Bitter National Magnet Laboratory, Massachusetts Institute of Technology, Cambridge, Massachusetts 02139, Department of Chemistry, Rijksuniversiteit te Leiden, NL-2300 RA Leiden, The Netherlands, and Department of Chemistry, Brandeis University, Waltham, Massachusetts 02254

Received March 3, 1992; Revised Manuscript Received June 9, 1992

ABSTRACT: Rotational resonance, a new solid-state NMR technique for determining internuclear distances, is used to measure a distance in the active site of bacteriorhodopsin (bR) that changes in different states of the protein. The experiments are targeted to the active site of bR through ^{13}C labeling of both the retinal chromophore and the Lys side chains of the protein. The time course of the rotor-driven magnetization exchange between a pair of ^{13}C nuclei is then observed to determine the dipolar coupling and therefore the internuclear distance. Using this approach, we have measured the distance from [14-^{13}C]retinal to [ε-^{13}C]Lys_{216} in dark-adapted bR in order to examine the structure of the retinal–protein linkage and its role in coupling the isomerizations of retinal to unidirectional proton transfer. This distance depends on the configuration of the intervening C=N bond. The 3.0 ± 0.2 Å distance observed in bR_{555} demonstrates that the C=N bond is syn, and the 4.1 ± 0.3 Å distance observed in bR_{568} demonstrates that the C=N bond is anti. These direct distance determinations independently confirm the configurations previously deduced from solid-state NMR chemical shift and resonance Raman vibrational spectra. The spectral selectivity of rotational resonance allows these two distances to be measured independently in a sample containing both bR_{555} and bR_{568}; the presence of both states and of 25% lipid in the sample demonstrates the use of rotational resonance to measure an active site distance in a membrane protein with an effective molecular mass of about 85 kDa. Rotational resonance experiments, such as this initial measurement of a retinal–protein distance, can be used to map the structure of the retinal binding pocket in the photocycle intermediates and therefore to elucidate the protein conformational changes involved in the mechanism of the proton pump.

Bacteriorhodopsin (bR)[1] is a membrane protein found in *Halobacterium halobium* which functions as a light-driven proton pump. Because bR is relatively small (26 kDa), stable, and abundant, it serves as an excellent model system for investigating the molecular basis of proton pumping and has been well-studied by a range of biophysical and biochemical techniques [for recent reviews, see Mathies et al., (1991), Birge, (1990) and Khorana (1988)].

The mechanism by which light energy drives the bR proton pump begins with the absorption of a photon by the *all-trans*-retinal chromophore, which is bound as a Schiff base to Lys_{216} of the protein. The light-driven isomerization of retinal to the 13-cis form is followed by a series of exothermic steps during which unidirectional proton transport occurs and the retinal reisomerizes to the all-trans state. Spectroscopic studies of the photocycle of the retinal chromophore have yielded a detailed picture of the kinetics of each step and the structure of retinal in each intermediate. The deprotonation and reprotonation of the retinal Schiff base in the formation and decay of the M intermediate is thought to be a key component of a proton-transfer chain across the membrane.

In recent years, investigations of the protein have begun to elucidate its role in the proton-pumping mechanism. For instance, site-directed mutagenesis experiments have identified amino acid residues critical to proton pumping (Mogi et al., 1988), and FTIR (Braiman et al., 1988; Eisenstein et al., 1987; Englehard et al., 1985) and solid-state NMR (Herzfeld et al., 1990; McDermott et al., 1991) studies have examined the protonation state of ionizable amino acids which may participate in a proton-transfer chain. Most recently, electron cryomicroscopy has resolved the aromatic side chains on the seven membrane-spanning α helices of bR, and a structural model for the protein has been proposed (Henderson et al., 1990).

Rotational resonance (R^2), a new solid-state NMR technique for measuring selected internuclear distances in polycrystalline or amorphous solids (Raleigh et al., 1988, 1989; Colombo et al., 1988; Levitt et al., 1990), can be used to

† This research was supported by the National Institutes of Health (GM-23289, GM-36810, RR-00995), The Netherlands Foundation for Chemical Research (SON), and The Netherlands Organization for the Advancement of Pure Science (NWO). L.K.T. was supported by a postdoctoral fellowship from the Jane Coffin Childs Memorial Fund for Medical Research and A.E.McD. was supported by a postdoctoral fellowship from the American Cancer Society (PF-3283).

‡ Massachusetts Institute of Technology.

§ Present address: Department of Chemistry, University of Massachusetts, Amherst, MA 01003.

∥ Present address: Department of Chemistry, Columbia University, New York, NY 10027.

⊥ Rijksuniversiteit te Leiden.

+ Brandeis University.

[1] Abbreviations: bR, bacteriorhodopsin; bR_{555}, component of dark-adapted bR with 13-*cis*-retinal; bR_{568}, light-adapted bR and component of dark-adapted bR with *all-trans*-retinal; CPMAS, cross-polarization magic angle spinning; FTIR, Fourier transform infrared spectroscopy; kDa, kilodaltons; MAS, magic angle spinning; NMR, nuclear magnetic resonance spectroscopy; R^2, rotational resonance; σ_{iso}, isotropic chemical shift; ν_r, magic angle spinning speed; T_2^{ZQ}, zero quantum T_2; δ and β are defined according to the conventions employed by Spiess (1978)—viz. σ_{iso} is the isotropic chemical shift, σ_{zz} is the shift tensor component furthest from σ_{iso}; $\delta = \sigma_{zz} - \sigma_{iso}$ is a breadth of the shift tensor, and β is the angle between σ_{zz} and the dipolar axis (the internuclear vector).

0006-2960/92/0431-7931$03.00/0

obtain a high-resolution picture of the retinal active site. Such structural information will ultimately be used to investigate the *coupling* between the retinal isomerizations and the unidirectional proton transfer across the membrane by examining how the active site structure changes in each step of the photocycle. Rotational resonance measures the homonuclear dipolar coupling in an isolated spin pair, which is proportional to $1/r^3$, where r is the internuclear distance. The dipolar coupling is normally averaged to zero by rapid tumbling in solution NMR or attenuated by magic angle spinning (MAS) in solid-state NMR. However, when a multiple of the MAS speed ($n\nu_r$) is chosen to match the frequency difference between two resonances ($\Delta\sigma_{iso} = n\nu_r$), the dipolar coupling is reintroduced. Because the MAS produces oscillations in the dipolar coupling at the same frequency as those produced by the chemical shift difference, the time-dependent dipolar coupling does not average to zero. This is known as the rotational resonance condition. Rotational resonance studies of small molecules have measured carbon–carbon distances of up to 5 ± 0.5 Å (Raleigh et al., 1989). The feasibility of such a study of bR has recently been demonstrated by a measurement of the distance between two retinal carbons in the protein, which bears on the mechanism of the opsin shift (Creuzet et al., 1991).

As a first step in investigating the coupling of the retinal isomerizations to proton transfer, we have measured a distance which probes the configuration of the Schiff base linking the chromophore to the protein. There are several ways in which the retinal C=N bond configuration may play a critical role in coupling. In contrast to the two stable states present in dark-adapted bR, the photocycle intermediates are *unstable*, presumably due to storage of the light energy which initiates the photocycle. This energy storage is critical to the coupling between the retinal isomerizations and proton pumping. A comparison of the structure of retinal in the low-energy forms present in the dark-adapted state with the structure in the high-energy photointermediates reveals two differences which may be involved in this energy storage, both of which are related to the configuration of the C=N bond. Both the directionality of the Schiff base N—H bond and the overall shape of the retinal polyene chain are similar in the 13-cis, 15-syn bR_{555} and the 13-trans, 15-anti bR_{568} configurations of dark-adapted bR [see Figure 1; Harbison et al. (1984)]. In contrast, resonance Raman spectra suggest that the high-energy intermediates, K, L, M, and N, have a 13-cis, 15-anti structure (Smith et al., 1984; Fodor et al., 1988; Ames et al., 1989), which alters both of the features (Figure 1). Thus the C=N bond configuration controls the environment of the Schiff base proton, which could alter its pK_a as part of the proton-pumping mechanism, and the steric interactions in the retinal pocket, which could induce protein conformational changes critical to driving proton transfer.

We have used rotational resonance to measure the distance between the 14-^{13}C of retinal and the ϵ-^{13}C of Lys_{216} in dark-adapted bR (indicated by * in Figure 1). These carbons flanking the Schiff base linkage are separated by three bonds, and the distance between them depends on whether the C=N bond is syn or anti. This distance measurement provides a direct determination of the configuration of the Schiff base linkage and serves as a first step in measuring retinal to protein distances to map the active site structure and conformationl changes in the photocycle.

EXPERIMENTAL PROCEDURES

Sample Preparation. [ϵ-^{13}C,^{15}N]Lys was synthesized as described previously (Raap et al., 1990). ϵ-^{15}N-Labeled Lys

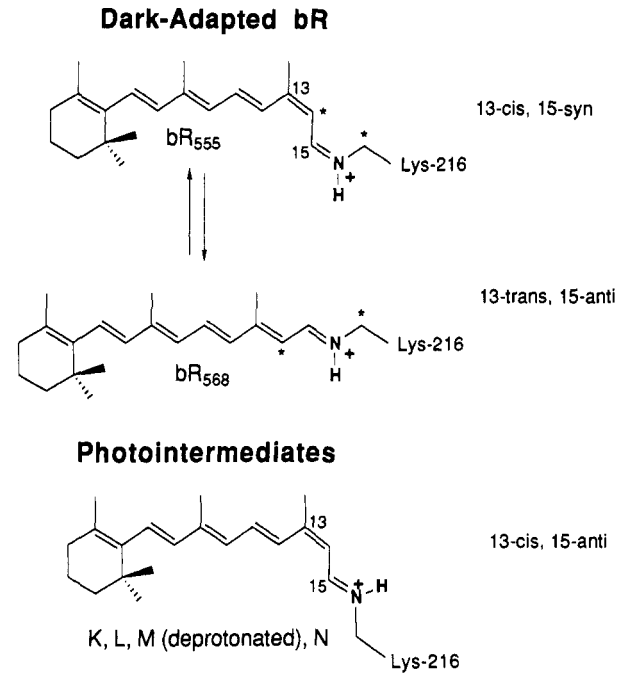

FIGURE 1: Proposed structures of retinal in dark-adapted bR and several photocycle intermediates. This paper reports the measurements of the distance between ^{13}C labels (*) at the 14-C of retinal and the ϵ-C of Lys_{216}, which depends on the configuration of the C=N bond.

was used in order to obtain narrower ϵ-^{13}C resonances, by removing quadrupolar broadening by the ^{14}N nucleus. The JW-3 strain of *Halobacterium halobium* was grown on a synthetic medium similar to that of Gochnauer and Kushner (1969), in which [ϵ-^{13}C,^{15}N]Lys was substituted for the unlabeled lysine, and the purple membrane was purified by the procedure of Oesterhelt and Stoeckenius (1973). The resulting [ϵ-^{13}C,^{15}N]Lys-bR sample was bleached in 0.5 M hydroxylamine hydrochloride, pH 8.1, to remove retinal. The bleaching was conducted overnight in darkness, at 35 °C and 1 mg/mL bR. The bleached bR membrane sample was washed three times in 50 mM HEPES buffer [*N*-2-(hydroxyethyl)piperazine-*N*'-2-ethanesulfonic acid], collecting the sample by centrifugation for 30 min at 30000*g* after each wash. After the final wash, the bleached sample was resuspended to 1 mg/mL in distilled water. The bR was then regenerated with [14-^{13}C]retinal, prepared by the method of Pardoen et al. (1984), by adding aliquots of retinal (dissolved at 1 mg/mL in dry ethanol) to the bR sample until the absorption spectrum indicated the regeneration was complete. The sample was then washed extensively to remove the excess retinal and retinal oxime: each wash consisted of resuspending the membranes in a solution of 2% bovine serum albumin and 1 mM NaN_3, incubation for 1–5 h, and subsequent centrifugation (30 min at 30000*g*). After 15 washes there was no detectable retinal oxime in the absorption spectrum; the sample was then washed extensively in 1 mM NaN_3 to remove the BSA.

NMR Spectroscopy and Data Analysis. Rotational resonance NMR spectra were collected on a home-built spectrometer with a ^{1}H frequency of 400 MHz. A home-built probe, utilizing a high-speed stator and 5-mm rotors (Doty Scientific, Columbia, SC), allowed MAS at speeds which satisfied the $n = 1$ rotational resonance condition (6–7 kHz). The rotational resonance pulse sequence depicted in Figure 2 utilized ^{1}H and ^{13}C 90° pulses of 5.5 and 6.6 μs, respectively, a 2-ms cross-polarization pulse, a 310-μs 180° pulse for the selective inversion, a 10-ms acquisition time, and a 3-s recycle

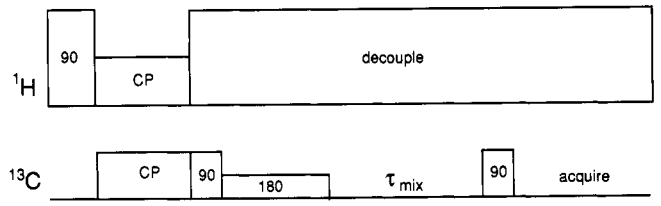

FIGURE 2: Pulse sequence used for rotational resonance experiments. The experiment begins with a standard cross-polarization sequence consisting of a 90° ^{1}H pulse, followed by simultaneous irradiation of both protons and carbons to transfer magnetization to carbon, and then decoupling of protons. After the carbon magnetization is prepared by cross polarization, the magnetization is stored along the z axis with a ^{13}C 90° pulse. One resonance is then inverted with a selective 180° pulse, centered at the appropriate Lys frequency. After a variable mixing time, τ_{mix}, during which rotational resonance-enhanced magnetization transfer occurs, a second 90° pulse returns the magnetization to the xy plane for observation.

delay. One data set collected with higher power (^{1}H 90° pulses of 4.1 μs) did not exhibit significantly narrower line widths or faster magnetization exchange, suggesting that the lower power (^{1}H 90° pulses of 5.5 μs) was sufficient for ^{1}H decoupling of this sample. The standard eight-phase cycle was supplemented by a four-phase cycling of the inversion pulse in order to cancel any partially inverted magnetization and avoid T_2 decay processes during the mixing time which would resemble magnetization exchange. Spectra were collected in sets of three to four mixing times including a 0 mixing time point (0.1 ms), which was used to normalize the data set. Approximately 7000–21 000 transients were accumulated for each mixing time; the total sample size was about 16 mg of bR (based on the absorbance at 560 nm). Because the purple membrane is only 75% bR, and the dark-adapted state consists of two conformations in a 60:40 ratio, this study represents the measurement of an active site distance in a membrane protein with an effective molecular mass of about 85 kDa.

CPMAS spectra (Figure 3) were collected on a 317-MHz home-built spectrometer, with a home-built MAS probe (7-mm Doty rotors), utilizing similar parameters except for a 3.8-μs ^{1}H 90° pulse.

The magnetization transfer data were analyzed by first subtracting the spectrum of an unlabeled sample. The center-band peak intensities (I_{14} and I_ϵ) were measured in the difference spectrum, and the calculated difference ($I_{14} - I_\epsilon$) was normalized to the value for the zero time point within each data set. The expected side-band peak intensities were negligible (within the noise) at the spinning speeds used in the rotational resonance experiments.

The percentage labeling of each site is quite important to this experiment. Any singly ^{13}C-labeled bR molecule cannot exchange and will contribute equally to the peak intensities at all mixing times and shift the exchange curve. This should affect the long mixing time points in particular; we observed that without correcting for the percent labeling the short and long time points would not both fit to a single calculated exchange curve for the bR_{555} data. We deduced from optical absorption spectra that roughly 15% of the bR retained its unlabeled retinal after bleaching. Thus, 15% of the Lys signal is from bR molecules which lack a ^{13}C label at the 14 position of retinal, and this Lys signal cannot exchange magnetization.[2] The data were corrected for this incomplete labeling by subtraction of 15% of the initial Lys signal from all of the Lys intensities (within each data set). These corrected data exhibited more consistent fits of both short and long mixing time points to a calculated curve. We also deduced that any

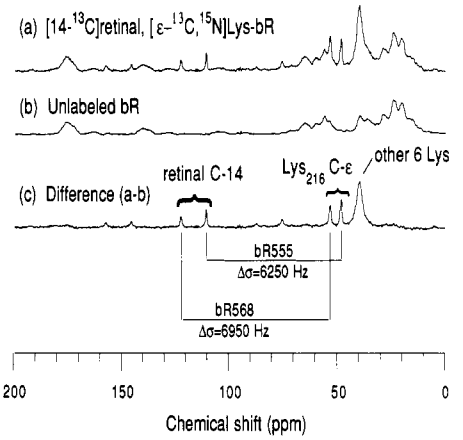

FIGURE 3: CPMAS difference spectroscopy of [14-^{13}C]retinal,[ϵ-^{13}C,^{15}N]Lys dark-adapted bR: ^{13}C spectra of (a) [14-^{13}C]-retinal,[ϵ-^{13}C,^{15}N]Lys-bR and of (b) unlabeled bR, both collected with a sample temperature of approximately –40 °C and a MAS speed of 2800 Hz (Farrar et al., in preparation). The difference spectrum (c) = (a) – (b) clearly displays the resonances of the retinal and Lys labels: six of the seven Lys in bR give rise to the largest peak at 40 ppm; Lys_{216}, which forms the Schiff base with retinal, gives rise to a pair of peaks at 48 and 53 ppm; and the retinal gives rise to the two downfield peaks at 110.5 and 122.5 ppm. For each of the two configurations of retinal present in the dark-adapted state, the corresponding 14-^{13}C and ϵ-^{13}C resonances and their chemical shift separation, $\Delta\sigma$, are indicated. Enhancement of magnetization exchange in the rotational resonance experiments was achieved by adjusting the magic angle spinning speed to match the chemical shift separation, $\nu_r = \Delta\sigma\,(n = 1)$, for each of the two retinal configurations.

error in this correction would not introduce a large uncertainty into the data—a maximum change in the measured distance of 0.2 Å.[3] However, in general it can be rather important to obtain an accurate determination of the percent labeling of the sample in rotational resonance experiments which measure distances between isotopic labels in proteins.

RESULTS

Solid-state NMR spectra of ^{13}C-labeled proteins are simplified by using difference spectroscopy (de Groot et al., 1988) to remove the background signals due to the 1% natural-abundance ^{13}C. The spectra in Figure 3, obtained using CP-MAS techniques together with difference spectroscopy, illustrate this approach. The top spectrum (Figure 3a) of dark-adapted doubly labeled [14-^{13}C]retinal,[ϵ-^{13}C,^{15}N]Lys-bR contains signals due to the labels and the natural-abundance ^{13}C background. Figure 3b is a spectrum of unlabeled bR

[2] Typical levels of Lys labeling (estimated by ^{3}H tracers) and the nearly complete disappearance of the [14-^{13}C]retinal peak in some experiments suggests that all of the [14-^{13}C]retinal nuclei have neighboring [ϵ-^{13}C]Lys nuclei. Thus we estimated that any incomplete labeling problems occurred at the 14-C nucleus (the [ϵ-^{13}C]Lys peak at long mixing times was never zero). Incomplete labeling at this site would be primarily due to incomplete bleaching of the bR membranes (the retinal synthesis produces 99% [14-^{13}C]retinal). The optical spectrum after bleaching suggested 15% of the bR retained its unlabeled retinal.

[3] The size of any error introduced by the correction for incomplete labeling was estimated as follows. The maximum possible correction corresponds to the assumption that all of the intensity remaining at the longest time point is due to incomplete labeling. We subtracted this minimum remaining intensity (for bR_{555} at the longest time point) from all points and compared the resulting magnetization exchange curve (maximum correction) with the uncorrected curve (minimum correction). The best fits to each of the two curves differed by only 0.2 Å. This indicates that our correction for incomplete labeling is not introducing a large uncertainty. The uncertainty would be larger for the measurement of a longer distance: because the exchange is slow, the peak intensities at long mixing times are not solely due to incomplete labeling, and the peak intensities at short mixing times are less diagnostic of the distance.

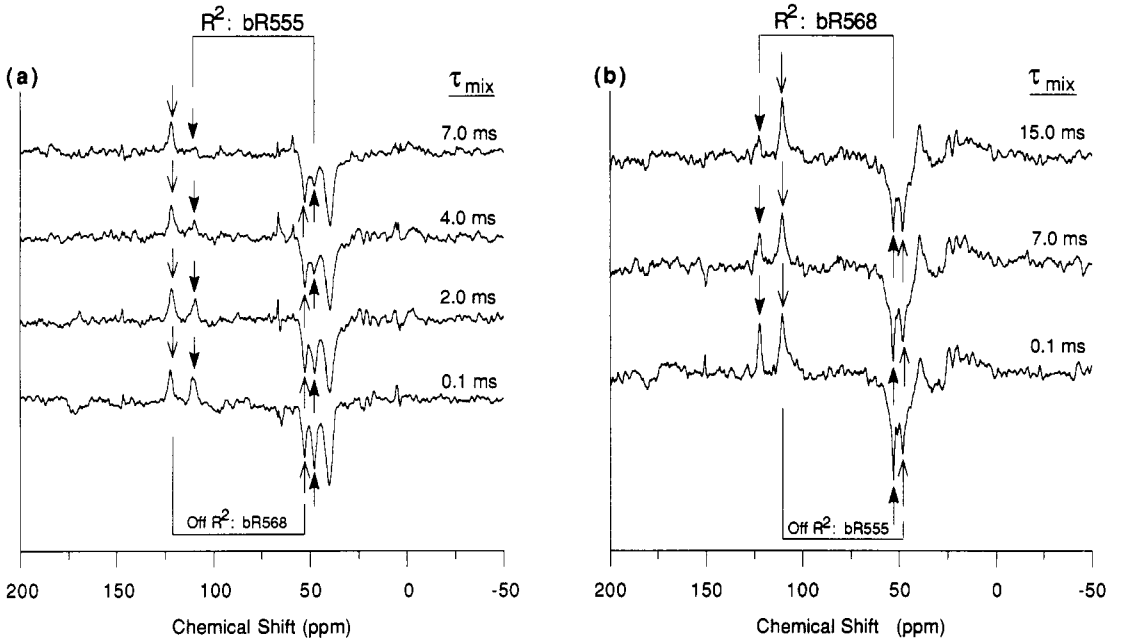

FIGURE 4: Rotational resonance difference spectra collected after magnetization exchange for various mixing times, τ_{mix}, as indicated. In each case, the upfield Lys region of the spectrum was selectively inverted with a weak pulse. The spectra were collected at a sample temperature of approximately −50 °C and MAS speeds which satisfy the rotational resonance condition for the indicated pair of resonances: (a) ν_r = 6240 Hz, which allows magnetization exchange in bR_{555}, and (b) ν_r = 6910 Hz, which allows magnetization exchange in bR_{568}. The peaks coupled by rotational resonance (filled arrowheads) decrease in intensity at increasing mixing times; the off-R^2 peaks (open arrowheads) remain constant in intensity, which indicates the selectivity of the rotational resonance-enhanced magnetization exchange. A comparison of the rotational resonance peak intensities for τ_{mix} = 7 ms demonstrates faster exchange (smaller remaining peak intensities) in the bR_{555} state, which indicates that the internuclear distance is shorter in bR_{555}.

obtained under the same conditions, in particular with the same spinning speed of 2.8 kHz. The difference spectrum, (c) = (a) − (b), exhibits only resonances due to the [14-^{13}C]-retinal and [ϵ-^{13}C]Lys labels (indicated by * in Figure 1). The most prominent resonance, at 40 ppm, has been assigned to the ϵ-^{13}C's of six of the seven Lys residues in the protein (Farrar et al., in preparation). The smaller upfield pair of resonances at 48 and 53 ppm is due to the ϵ-^{13}C of Lys_{216} and the downfield pair of resonances arise from the 14-^{13}C of retinal. The upfield line of each of these pairs of resonances corresponds to the bR_{555} form present in the dark-adapted state; they are shifted upfield relative to the bR_{568} form due to a steric interaction (γ effect) between the protons on the ϵ-C of Lys_{216} and the proton on the 14-C of retinal [Harbison et al. (1984) and Farrar et al., in preparation].

Figure 3 also illustrates the spinning speeds (ν_r) required to match the chemical shift differences ($\Delta\sigma_{iso}$) and satisfy the rotational resonance condition needed to drive magnetization transfer:

$$\Delta\sigma_{iso} = n\nu_r$$

Rotational resonance experiments on the bR_{555} component of dark-adapted bR, with resonances at 110.5 (14-^{13}C) and 48 ppm (ϵ-^{13}C), require ν_r = 6250 Hz ($\Delta\sigma_{iso}$ = 62.5 ppm, for n = 1 and a ^{13}C frequency of 100 MHz). The corresponding experiments on the bR_{568} component of dark-adapted bR, with resonances at 122.5 (14-^{13}C) and 53 ppm (ϵ-^{13}C), require ν_r = 6950 Hz ($\Delta\sigma_{iso}$ = 69.5 ppm). Thus the spinning speeds required to satisfy rotational resonance for the two components of dark-adapted bR differ by 700 Hz. This difference is significantly larger than the width of the rotational resonance condition, which is on the order of the line width of the resonances (each about 130 Hz). Therefore, we can use rotational resonance to *selectively* drive magnetization exchange in either bR_{555} or bR_{568}, and measure the distance in each form of dark-adapted bR, without interference from the presence of the other. This selectivity also permits us to use the off-R^2 peaks as a control: their intensities should remain constant while the on-R^2 peaks undergo magnetization exchange.

Rotational resonance difference spectra of bR, obtained with the pulse sequence depicted in Figure 2 for several representative mixing times, are shown in Figure 4. The [ϵ-^{13}C]Lys peak was inverted because of its smaller chemical shift anisotropy. The MAS speeds were chosen to satisfy the rotational resonance condition for the bR_{555} component (Figure 4a) and for the bR_{568} component (Figure 4b). In both cases it is clear that the on-R^2 peak intensities (filled arrowheads) decrease as the mixing time increases, while the off-R^2 peak intensities (open arrowheads) remain relatively constant. Furthermore, a comparison of the on-R^2 peak intensities for the 7-ms mixing time for the two forms of bR shows more rapid exchange (smaller remaining intensities) for bR_{555} than for bR_{568}, indicating a significantly shorter distance in bR_{555}.

The differences in exchange behavior for the on- and off-R^2 peaks and for the two forms of bR present in the dark-adapted state are clear in Figure 5, which is a plot of the difference in peak intensity (I_{14} - I_ϵ) as a function of mixing time. The off-R^2 peaks (▲) are not undergoing magnetization exchange on this time scale. The scatter in these points is representative of the experimental error in the peak intensity measurements; a similar degree of scatter is also observed in the on-R^2 points. Despite the scatter in the data it is quite apparent that the magnetization exchange curves for the two forms of bR are significantly different. The more rapid exchange observed in bR_{555} indicates a stronger dipolar coupling due to a shorter internuclear distance, consistent with prior evidence that C=N is syn in bR_{555} and anti in bR_{568}.

Computer simulations of the magnetization exchange behavior expected for various distances [described in detail by Levitt et al. (1990) and Creuzet et al. (1992)], using parameters appropriate for these nuclei (discussed below) were

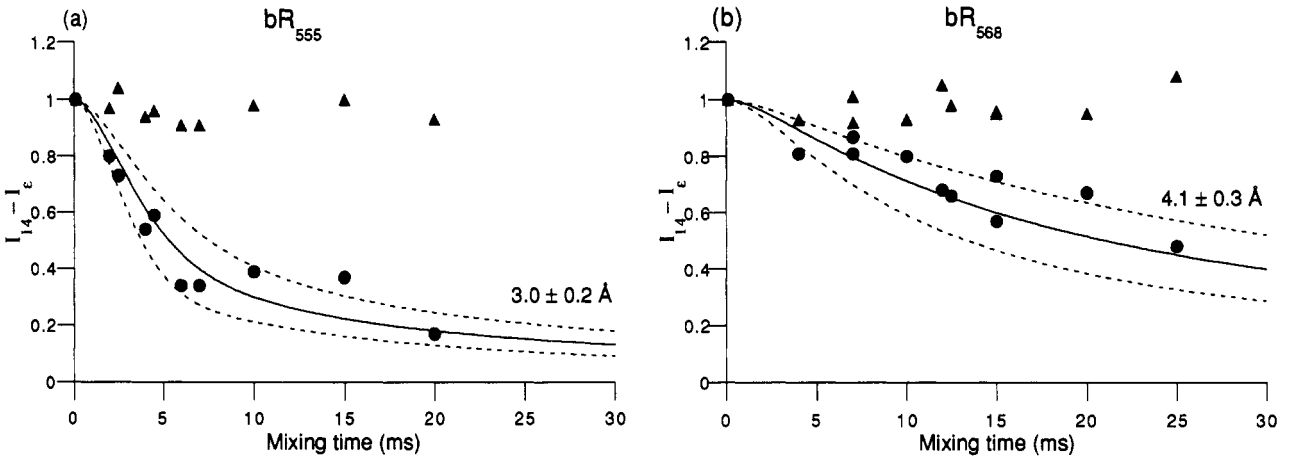

FIGURE 5: Magnetization exchange data and simulations for the bR_{555} and bR_{568} components of dark-adapted bR. The difference in peak intensities (I_{14} - I_{ϵ}, normalized to its value at zero mixing time) is plotted as a function of the mixing time for both the on-R^2 (●) and off-R^2 (▲) resonances. The small variation in the off-R^2 points demonstrates the experimental scatter in the data and indicates that no appreciable decrease in peak intensities occurs on this time scale other than the rotational resonance-enhanced magnetization exchange. The solid and dashed lines are the calculated magnetization exchange curves for the indicated distances. For bR_{555} (a), the comparison between the data and the calculated exchange curves indicates a distance of 3.0 Å (solid line). The most extreme distances which can provide an adequate fit within the scatter in the data are 2.8 and 3.2 Å (dashed lines); thus we estimate an uncertainty of ±0.2 Å in this distance measurement. For bR_{568} (b), the comparison between the data and the calculated exchange curves indicates a distance of 4.1 Å (solid line). The most extreme distances which can provide an adequate fit within the scatter in the data are 3.8 and 4.4 Å (dashed lines); thus we estimate an uncertainty of ±0.3 Å in this distance measurement.

used to determine the distances in bR_{555} and bR_{568}. The solid lines in Figure 5 represent a visual best fit to the experimental data; the dashed lines represent the most extreme fits which could fit the scatter in the data, to provide an estimate of the error in the distance measurement. The 14-^{13}C to ϵ-^{13}C distance is 3.0 ± 0.2 Å in bR_{555} and 4.1 ± 0.3 Å in bR_{568}. These distances are similar to those predicted by energy minimization using CHARMm (Polygen Corp.) for the syn (3.1 Å) and anti (3.9 Å) configurations of the C=N bond.

DISCUSSION

Rotational Resonance Distance Measurements: Parameters Influencing Simulations of Magnetization Exchange Curves. Magnetization exchange behavior can be interpreted qualitatively to yield insight into relative distances (closer in bR_{555} than in bR_{568}) and can also be analyzed quantitatively to determine the dipolar couplings which yield the distances. Computer simulations of the magnetization exchange behavior depend on a number of parameters which can be measured or estimated: the zero quantum T_2 (T_2^{ZQ}), the chemical shift tensor of each ^{13}C, and the relative orientation of the two tensors can influence the magnetization exchange. The effects of these parameters on our experiments are discussed below, in order to illustrate the errors which arise from each for this case, as well as for general applications of rotational resonance.

The shape of the magnetization exchange curve depends most strongly on the relative magnitudes of the dipolar coupling, which determines the frequency of the oscillation of magnetization between the two nuclei, and the zero quantum T_2, which damps this oscillatory behavior. The damping of the magnetization exchange is due to dephasing off of the rotational resonance condition, at a rate $1/T_2^{ZQ}$, which can be estimated as the sum of the independent dephasing rates of each spin (see below). If the dipolar coupling is much larger than $1/T_2^{ZQ}$, the magnetization undergoes a damped oscillation between the two nuclei, as observed for directly bonded ^{13}C in Zn acetate (Raleigh et al., 1988). For longer distances, with smaller dipolar couplings, $1/T_2^{ZQ}$ dominates and the magnetization exchange curve approaches a monotonic decay, as observed for two ^{13}C nuclei separated by 5 Å in tyrosine ethyl ester (Raleigh et al., 1989). The observed nonoscillatory curves in dark-adapted bR are consistent with the predicted 14-^{13}C to ϵ-^{13}C distances of 3–4 Å.

The importance of T_2^{ZQ} and the other parameters in the computer simulation can be illustrated by contour plots of the difference between the calculated and the experimental exchange curves as a function of two parameters of the simulation. The contour plots shown in Figure 6 illustrate the significance of various parameters for the simulation of the magnetization exchange curve to obtain a distance. Each plot shows the effect of a parameter (vertical axis) on the dipolar coupling (horizontal axis). The shaded area represents the minimum contour level, a root mean square deviation of $\leq$0.08 between calculated and experimental values. Panels a and b of Figure 6 show the dependence of the dipolar coupling on T_2^{ZQ}, for bR_{555} and bR_{568}, respectively. Although this parameter has quite a large effect on the dipolar coupling, there is no overlap between the minimum contour areas for the two configurations of retinal in dark-adapted bR. The two distances can be distinguished independent of any knowledge of T_2^{ZQ}. However, the broad range of dipolar couplings (horizontal spread) of the minima in these contour plots indicates that estimating T_2^{ZQ} is critical to quantiative distance measurements. Creuzet et al. (1992) have shown that estimates based on the line widths, $(T_2^{ZQ})^{-1} = (T_2^{(1)})^{-1} + (T_2^{(2)})^{-1}$, are reliable for obtaining accurate distances from simulations of rotational resonance data. We estimated T_2^{ZQ} = 1.1–1.7 ms from the 14-^{13}C and ϵ-^{13}C line widths. This range of T_2^{ZQ} values yields a range of distances of 2.8–3.1 Å in bR_{555} and 4.0–4.6 Å in bR_{568} (crosshatched areas), in agreement with the 3.1- and 3.9-Å distances predicted by CHARMm.

Another potentially influential parameter is the chemical shift tensor of each carbon. The larger 14-^{13}C tensor should have a significant effect; our calculations utilized the 14-^{13}C chemical shift tensor values determined in bR from side-band intensities in MAS experiments (Harbison et al., 1984; Smith et al., 1989) by the method of Herzfeld and Berger (1980).

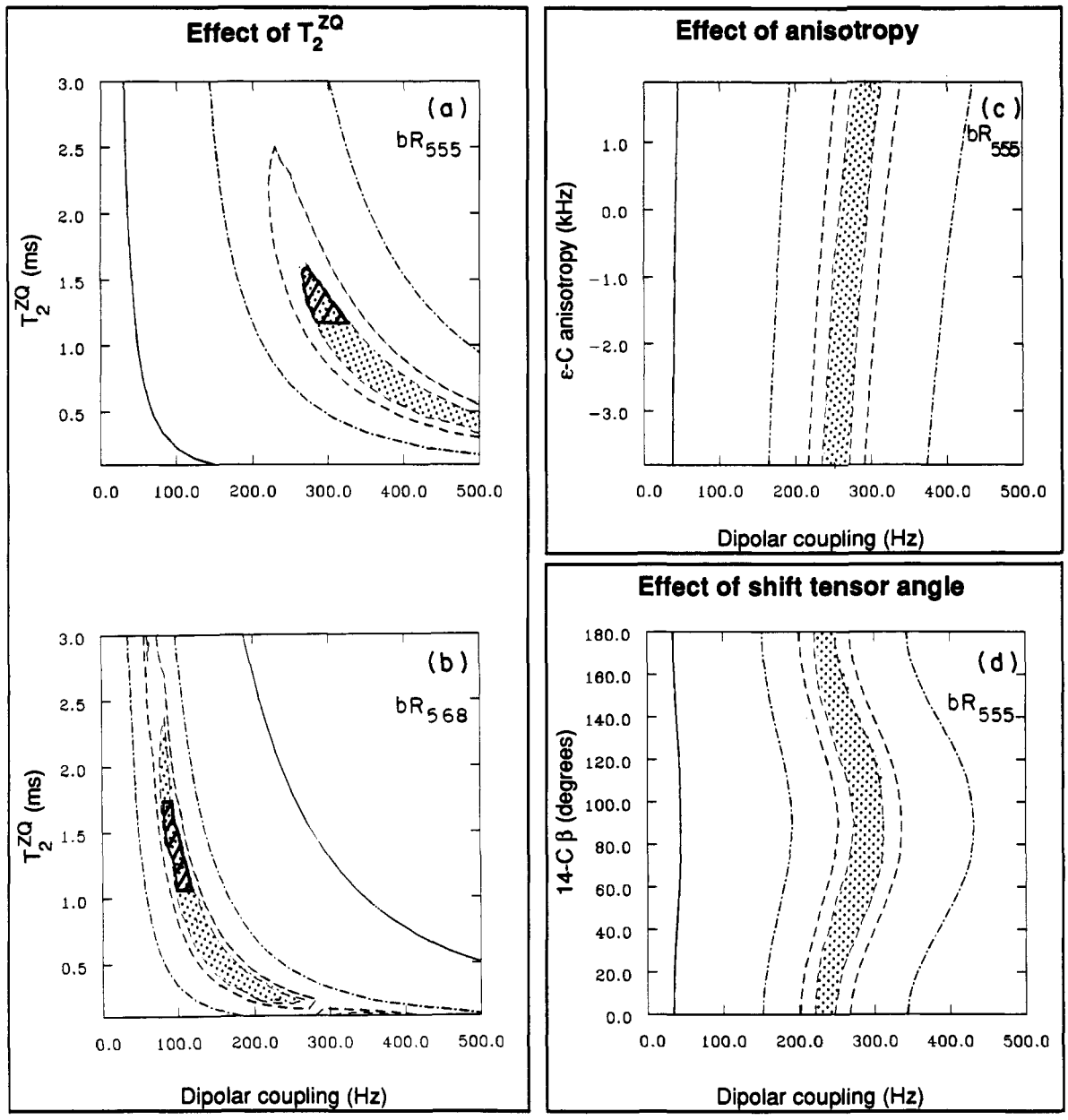

FIGURE 6: Contour plots of the dependence of the difference between calculated and experimental exchange curves on the dipolar coupling and another parameter used for the calculation. The area of minimum deviation (root mean square deviation ≤0.08) between calculated and experimental exchange is shaded (other plotted contours are 0.1, 0.2, and 0.5 root mean square deviation). The effect of the T_2^{ZQ} on the best fit (plot a for bR_{555} and plot b for bR_{568}) is significant: in the absence of an accurate estimate of T_2^{ZQ}, the data fit to a large range of dipolar couplings and corresponding distances, but the two configurations are still clearly distinguishable (shaded areas do not overlap). The estimated T_2^{ZQ} = 1.1–1.7 ms restricts the fit to a distance range of 2.8–3.1 Å for bR_{555} and 4.0–4.6 Å for bR_{568} (crosshatched areas). Plot c shows the effect of the ϵ-^{13}C shift anisotropy on the best fit of the dipolar coupling for bR_{555}. Small shift tensors such as that of ϵ-^{13}C have little effect on the exchange: allowing δ to vary between −3800 and 1900 Hz yields a corresponding distance range of only ±0.2 Å. Plot d illustrates the fact that knowledge of the angles between the shift tensors is unnecessary for obtaining an accurate distance, for the $n = 1$ rotational resonance: the full range of values of the most significant angle β (beteen σ_{zz} and the internuclear vector) yields a best fit distance range of only ±0.2 Å for bR_{555}.

In contrast, the small ϵ-^{13}C tensor is very difficult to measure in bR, but may be small enough to be insignificant. Two extreme values for the anisotropy (δ, the breadth of the chemical shift tensor) of methylene carbons with similar isotropic chemical shifts are δ = −3800 (ethanol) and δ = 1900 (glycine). Contour plots can be used to estimate how much this range of anisotropy values will influence the calculated distance. Figure 6c plots the effect of δ_ϵ in this range on the dipolar coupling in bR_{555}; the minimum contour level corresponds to a distance range of 2.8–3.2 Å. On the basis of such contour plots, we conclude that the value of the small Lys shift tensor has a relatively small effect on the distance measured by rotational resonance.

Finally, the relative orientations of the two chemical shift tensors are additional parameters used in the magnetization exchange simulation. Figure 6D shows the effect of the most significant angle β, between σ_{zz} (the 14-^{13}C chemical shift tensor component furthest shifted from the isotropic chemical shift) and the dipolar axis (the internuclear vector), on the dipolar coupling in bR_{555}. In this particular experiment, our knowledge of the geometry of retinal and the orientations of shift tensor axes in double-bonded systems (Wolff et al., 1977) permits us to deduce that β = 90° for both bR_{555} and bR_{568}. However, as is illustrated in Figure 6d, this parameter has a relatively weak effect for the $n = 1$ resonance, yielding an error range of ±0.2 Å for the same minimum contour level.

On the other hand, for "higher order" rotational resonances ($n > 1$ in $\Delta\sigma_{iso} = n\nu_r$) exchange depends more strongly on the relative orientations of the shift tensors (Levitt et al., 1990).

In summary, the contour plots illustrate the relative sensitivity of the simulations of magnetization exchange curves to various parameters. Accurate estimates of T_2^{ZQ} and large ^{13}C shift anisotropies (which can be determined experimentally) are essential to obtain an accurate distance, whereas the remaining parameters are relatively unimportant. On the basis of contour plots, we have estimated that the errors due to each parameter and to our estimate of the percentage labeling (see Experimental Procedures) are each of the same or smaller magnitude than the error due to the scatter in the experimental data. These error estimates are difficult to combine quantitatively into an overall error in the distance measurement but illustrate the potential and limitations of the technique. At this stage of devleopment, rotational resonance studies of complex macromolecules can *clearly* distinguish two conformations with ^{13}C–^{13}C distances differing by $\approx$1 Å [this work and Creuzet et al. (1990)]. Improvements in signal-to-noise ratios may decrease the current ±0.3 Å error limitations and permit measurments of vary small changes in distance. Rotational resonance is therefore expected to be a useful approach for studying a variety of protein conformational changes.

Structure of the Retinal–Protein Schiff Base Linkage in bR. The retinal 14-^{13}C to Lys_{216} ϵ-^{13}C distance we have measured is a direct and unambiguous determination of the configuration of the retinal– protein Schiff base linkage. Our results confirm the conclusions of previous studies which deduced the configuration of the C=N bond from the 14-^{13}C chemical shifts (Harbison et al., 1984), from the ϵ-^{13}C chemical shifts (Farrar et al., in preparation), and from resonance Raman spectroscopy (Smith et al., 1984). These less direct methods are not always unambiguous: for instance, a chemical shift interpretation which assigned a photointermediate to be a syn M state (Smith et al., 1989a) is currently being reevaluated. On the other hand, the accuracy of our measurement is insufficient to rule out small twists about the C=N bond (a 45° twist should change the 14-^{13}C to ϵ-^{13}C distance by less than 0.2 Å), underlining the need to apply a range of techniques to determine the structure of retinal during the bR photocycle. Rotational resonance distance measurements will be a powerful direct probe for determining the retinal conformation in cryotrapped photointermediates, which will facilitate comparison between studies of photocycle intermediates by different biophysical methods. Characterization of the trapped M intermediate(s) with rotational resonance distance measurements is in progress.

Comparison of the retinal structures in the stable states present in dark-adapted bR suggests that the retinal binding site is designed to accommodate a fairly linear chromophore, as is present in the all-trans bR_{568} and 13-cis, 15-syn bR_{555} states (Harbison et al., 1984). There are likely to be unfavorable interactions between the bent 13-cis, 15-anti chromophore structures present in the high-energy intermediates K, L, M, and N and protein residues in the chromophore binding pocket. As has been proposed in a recent model (Fodor et al., 1988), these interactions may be used to drive protein conformational changes which alter the Schiff base environment in order to provide both the driving force and the directionality of the pumping mechanism. Rotational resonance provides a powerful new approach for measuring the retinal–protein distances required to delineate the protein conformational changes involved in coupling the retinal photocycle to unidirectional proton transfer.

CONCLUSION

We have used rotational resonance, a new solid-state NMR technique which measures homonuclear dipolar couplings, to directly measure a conformational change in the active site of a membrane protein with an effective molecular mass of 85 kDa. The retinal 14-^{13}C to Lys_{216} ϵ-^{13}C distances that we have measured in the two forms of dark-adapted bR provide independent verification of the configuration of the C=N bond, which had been predicted by both resonance Raman and NMR chemical shift data: the 3.0 ± 0.2 Å distance in bR_{555} determines the C=N configuration to be syn, and the 4.1 ± 0.3 Å distance in bR_{568} determines the C=N configuration to be anti.

Future experiments will measure this and other retinal–protein distances in various bR photocycle intermediates, with the goal of elucidating the structural changes in the retinal active site to determine how the retinal photocycle is coupled to proton pumping. Rotational resonance promises to be an important general tool for probing active site structure and conformational changes involved in molecular mechanisms of membrane protein function.

ACKNOWLEDGMENT

We thank A. Thakkar for technical assistance with the high-speed probe and numerous others at the FBNML for assistance with instrumentation and software and for helpful discussions.

REFERENCES

Ames, J. B., Fodor, S. P. A., Gebhard, R., van den Berg, E. M. M., Lugtenberg, J., & Mathies, R. A. (1989) *Biochemistry 28*, 3681.

Birge, R. R. (1990) *Biochim. Biophys. Acta 1016*, 293.

Braiman, M. S., Mogi, T., Marti, T., Stern, L. J., Khorana, H. G., & Rothschild, K. J. (1988) *Biochemistry 27*, 8516.

Colombo, M. G., Meier, B. H., & Ernst, R. R. (1988) *Chem. Phys. Lett. 146*, 189.

Creuzet, F., McDermott, A., Gebhard, R., ven der Hoef, K., Spijker-Assink, M. B., Herzfeld, J., Lugtenburg, J., Levitt, M. H., & Griffin, R. G. (1991) *Science 251*, 783.

Creuzet, F., Raleigh, D. P., Levitt, M. H., & Griffin, R. G. (1992) *J. Am. Chem. Soc.* (in press).

de Groot, H. J. M., Copié, V., Smith, S. O., Allen, P. J., Winkel, C., Lugtenburg, J., Herzfeld, J., & Griffin, R. G. (1988) *J. Magn. Reson. 77*, 251.

Eisenstein, L., Lin, S.-L., Dollinger, G., Odashima, K., Termini, J., Konno, K., Ding, W.-D., & Nakanishi, K. (1987) *J. Am. Chem. Soc. 109*, 6860.

Englehard, M., Gerwert, K., Hess, B., Kreutz, W., & Siebert, F. (1985) *Biochemistry 24*, 400.

Fodor, S. P. A., Ames, J. B., Gebhard, R., van den Berg, E. M. M., Stoeckinius, W., Lugtenberg, J., & Mathies, R. A. (1988) *Biochemistry 27*, 7097.

Gochnauer, M. B., & Kushner, D. J. (1969) *Can. J. Microbiol. 15*, 1157.

Harbison, G. S., Smith, S. O., Pardoen, J. A., Mulder, P. P. J., Lugtenburg, J., Herzfeld, J., Mathies, R. A., & Griffin, R. G. (1984) *Proc. Natl. Acad. Sci. U.S.A. 81*, 1706.

Henderson, R., Baldwin, J. M., Ceska, T. A., Zemlim, F., Beckmann, E., & Downing, K. H. (1990) *J. Mol. Biol. 213*, 899.

Herzfeld, J., & Berger, A. E. (1980) *J. Chem. Phys. 73*, 6021.

Herzfeld, J., Das Gupta, S. K., Farrar, M. R., Harbison, G. S., McDermott, A. E., Pelletier, S. L., Raleigh, D. P., Smith, S. O., Winkel, C., Lugtenburg, J., & Griffin, R. G. (1990) *Biochemistry 29*, 5567.

Khorana, H. G. (1988) *J. Biol. Chem. 263*, 7439.

Levitt, M. H., Raleigh, D. P., Creuzet, F., & Griffin, R. G. (1990) *J. Chem. Phys. 92*, 6347.

Mathies, R. A., Lin, S. W., Ames, J. B., & Pollard, W. T. (1991) *Annu. Rev. Biophys. Biophys. Chem. 20*, 491.

McDermott, A. E., Thompson, L. K., Winkel, C., Farrar, M. R., Pelletier, S., Lugtenburg, J., Herzfeld, J., & Griffin, R. G. (1991) *Biochemistry 30*, 8366.

Mogi, T., Stern, L. J., Marti, T., Chao, B. H., & Khorana, H. G. (1988) *Proc. Natl. Acad. Sci U.S.A. 85*, 4148.

Oesterhelt, D., & Stoeckenius, W. (1973) *Methods Enzymol. 31*, 667.

Pardoen, J. A., Winkel, C., Mulder, P. P. J., & Lugtenburg, J. (1984) *Recl. Trav. Chim. Pays-Bas 103*, 135.

Raap, J., van der Wielen, C. M., & Lugtenburg, J. (1990) *Recl. Trav. Chim. Pays-Bas 109*, 277.

Raleigh, D. P., Levitt, M. H., & Griffin, R. G. (1988) *Chem. Phys. Lett. 146*, 71.

Raleigh, D. P., Creuzet, F., Das Gupta, S. K., Levitt, M. H., & Griffin, R. G. (1989) *J. Am. Chem. Soc. 111*, 4502.

Smith, S. O., Hornung, I., van der Steen, R., Pardoen, J. A., Braiman, M. S., Lugtenburg, J., & Mathies, R. A. (1984) *Proc. Natl. Acad. Sci. U.S.A. 81*, 2055.

Smith, S. O., Courtin, J., van den Berg, E., Winkel, C., Lugtenburg, J., Herzfeld, J., & Griffin, R. G. (1989a) *Biochemistry 28*, 237.

Smith, S. O., de Groot, H. J. M., Gebhard, R., Courtin, J. M. L., Lugtenburg, J., Herzfeld, J., & Griffin, R. G. (1989b) *Biochemistry 28*, 8897.

Spiess, H. W. (1978) in *NMR Basic Principles and Progress* (Diehl, P., Fluck, E., & Klosfield, C., Eds.) Spreinger, Berlin.

Wolff, E. K., Griffin, R. G., & Waugh, J. S. (1977) *J. Chem. Phys. 67*, 2387.